Forum Geometricorum
Volume 11 (2011) 183–199.

FORUM GEOM
ISSN 1534-1178

The Lemniscatic Chessboard

Joel C. Langer and David A. Singer

Abstract. Unit speed parameterization of the lemniscate of Bernoulli is given by a simple rational expression in the lemniscatic sine function. The beautiful structure of this parameterization becomes fully visible only when complex values of the arclength parameter are allowed and the lemniscate is viewed as a complex curve. To visualize such hidden structure, we will show squares turned to spheres, chessboards to lemniscatic chessboards.

1. Introduction

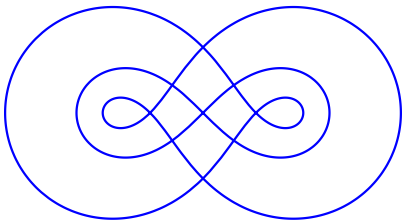

Figure 1. The lemniscate and two parallels.

The lemniscate of Bernoulli resembles the iconic notation for infinity ∞. The story of the remarkable discoveries relating elliptic functions, algebra, and number theory to this plane curve has been well told but sparsely illustrated. We aim to fill the visual void.

Figure 1 is a plot of the lemniscate, together with a pair of *parallel curves*. Let $\gamma(s) = x(s) + iy(s),\ 0 \le s \le L$, parameterize the lemniscate by arclength, as a curve in the complex plane. Then analytic continuation of $\gamma(s)$ yields parameterizations of the two shown parallel curves: $\gamma_\pm(s) = \gamma(s \pm iL/16),\ 0 \le s \le L$. Let $p_1, \dots, p_9$ denote the visible points of intersection. The figure and the following accompanying statements hint at the beautiful structure of $\gamma(s)$:

- The intersection at each p_j is orthogonal.
- The arclength from origin to closest point of intersection is $L/16$.
- Each point p_j is constructible by ruler and compass.

We briefly recall the definition of the lemniscate and the *lemniscatic integral*. Let $\mathcal{H}$ denote the rectangular hyperbola with foci $h_\pm = \pm\sqrt{2}$. Rectangular and

Publication Date: September 21, 2011. Communicating Editor: Paul Yiu.

polar equations of $\mathcal{H}$ are given by:

$$\begin{aligned} 1 &= x^2 - y^2 \\ 1 &= r^2\cos^2\theta - r^2\sin^2\theta = r^2\cos 2\theta \end{aligned}$$

Circle inversion, $(r,\theta) \mapsto (1/r,\theta)$, transforms $\mathcal{H}$ into the Bernoulli lemniscate $\mathcal{B}$:

$$\begin{aligned} r^4 &= r^2\cos 2\theta \\ (x^2+y^2)^2 &= x^2 - y^2 \end{aligned}$$

The foci of $\mathcal{H}$ are carried to the *foci* $b_\pm = \pm 1/\sqrt{2}$ of $\mathcal{B}$. While focal distances for the hyperbola $d_\pm(h) = \|h - h_\pm\|$ have constant difference $|d_+ - d_-| = 2$, focal distances for the lemniscate $d_\pm(b) = \|b - b_\pm\|$ have constant product $d_+ d_- = 1/2$. (Other constant values of the product $d_+ d_- = d^2$ define the non-singular Cassinian ovals in the confocal family to $\mathcal{B}$.)

Differentiation of the equation $r^2 = \cos 2\theta$ and elimination of $d\theta$ in the arclength element $ds^2 = dr^2 + r^2 d\theta^2$ leads to the elliptic integral for arclength along $\mathcal{B}$:

$$s(r) = \int \frac{dr}{\sqrt{1-r^4}} \tag{1}$$

The length of the full lemniscate $L = 4K$ is *four* times the complete elliptic integral $\int_0^1 dr/\sqrt{1-r^4} = K \approx 1.311$. One may compare K, formally, to the integral for arclength of a quarter-circle $\int_0^1 dx/\sqrt{1-x^2} = \frac{\pi}{2}$, though the integral in the latter case is based on the rectangular equation $y = \sqrt{1-x^2}$.

The lemniscatic integral $s(r)$ was considered by James Bernoulli (1694) in his study of elastic rods, and was later the focus of investigations by Count Fagnano (1718) and Euler (1751) which paved the way for the general theory of elliptic integrals and elliptic functions. In particular, Fagnano had set the stage with his discovery of methods for *doubling an arc* of $\mathcal{B}$ and subdivision of a quadrant of $\mathcal{B}$ into two, three, or five equal (length) sub-arcs by ruler and compass constructions; such results were understood via addition formulas for elliptic integrals and (ultimately) elliptic functions.

But a century passed before Abel (1827) presented a proof of the definitive result on subdivision of $\mathcal{B}$. Abel's result followed the construction of the 17-gon by Gauss (1796), who also showed that the circle can be divided into n equal parts when $n = 2^j p_1 p_2 \dots p_k$, where the integers $p_i = 2^{2^{m_i}} + 1$ are distinct *Fermat primes*. Armed with his extensive new theory of elliptic functions, Abel showed: *The lemniscate can be n-subdivided for the very same integers $n = 2^j p_1 p_2 \dots p_k$.* (See [3], [11], [10] and [13].)

2. Squaring the circle

It may seem curious at first to consider complex values of the "radius" r in the lemniscatic integral, but this is essential to understanding the integral's remarkable properties. Let $D = \{w = x + iy : x^2 + y^2 < 1\}$ be the open unit disk in the

complex w-plane and, for each $w \in D$, consider the radial path $r = tw, 0 \le t \le 1$. The complex line integral

$$\zeta = s(w) = \int_0^w \frac{dr}{\sqrt{1-r^4}} = \int_0^1 \frac{w\,dt}{\sqrt{1-w^4t^4}} \tag{2}$$

defines a complex analytic function on D. (Here, $\sqrt{1-r^4}$ denotes the analytic branch with $\mathrm{Re}[\sqrt{1-r^4}] > 0$, for $r \in D$.) Then $s(w)$ maps D one-to-one and conformally onto the open square $\mathcal{S}$ with vertices $\pm K, \pm iK$—*the lemniscatic integral squares the circle!*

In fact, for $n = 3, 4, \ldots$, the integral $s_n(w) = \int_0^w \frac{dr}{(1-r^n)^{2/n}}$ maps D conformally onto the regular n-gon with vertices $\sigma_n^k = e^{2\pi ki/n}$. This is a beautifully symmetrical (therefore tractable) example in the theory of the *Schwarz-Christoffel mapping*. Without recalling the general theory, it is not hard to sketch a proof of the above claim; for convenience, we restrict our discussion to the present case $n = 4$.

First, $s(w)$ extends analytically by the same formula to the unit circle, except at $\pm 1, \pm i$, where $s(w)$ extends continuously with values $s(e^{\pi ki/2}) = i^k K,\ k = 0, 1, 2, 3$. The four points $e^{\pi ki/2}$ divide the unit circle into four quarters, whose images $\gamma(t) = s(e^{it})$ we wish to determine. Differentiation of $\gamma'(t) = ie^{it}/\sqrt{1-e^{4it}}$ leads, after simplification, to $\gamma''(t)/\gamma'(t) = \cot 2t$. Since this is real, it follows that the velocity and acceleration vectors are parallel (or anti-parallel) along $\gamma(t)$, which is therefore locally straight. Apparently, s maps the unit circle to the square $\mathcal{S}$ with vertices $i^k K$, where the square root type singularities of $s(w)$ turn circular arcs into right angle bends. Standard principles of complex variable theory then show that D must be conformally mapped onto $\mathcal{S}$—see Figure 2.

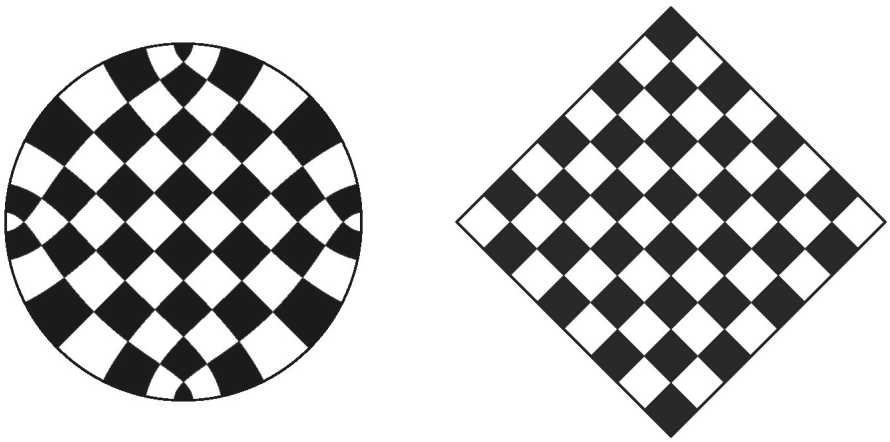

Figure 2. The lemniscatic integral $s(w) = \int_0^w \frac{dr}{\sqrt{1-r^4}}$ squares the circle.

The 64 subregions of the *circular chessboard* of Figure 2 (left) are the preimages of the squares in the standard chessboard (right). Four of the subregions in the disk appear to have only three sides apiece, but the bounding arcs on the unit circle each count as two sides, bisected by vertices $\pm 1, \pm i$.

It is visually obvious that the circular and standard chessboards have precisely the same symmetry—namely, that of a square. To be explicit, the mapping $\zeta = s(w)$ is easily seen to be equivariant with respect to the four rotations and four reflections of the dihedral group D_4:

$$s(i^k w) = i^k s(w), \quad s(i^k \bar{w}) = i^k \overline{s(w)}, \quad k = 0, 1, 2, 3. \tag{3}$$

Anticipating the next section, we note that the conformal map $\zeta = s(w)$ inverts to a function $w = s^{-1}(\zeta)$ which maps standard to circular chessboard and is also D_4-equivariant.

3. The lemniscatic functions

Let us return briefly to the analogy between arclength integrals for lemniscate and circle. The integral $t = \int dx/\sqrt{1-x^2}$ defines a monotone increasing function called $\arcsin x$ on the interval $[-1, 1]$. By a standard approach, $\sin t$ may be defined, first on the interval $[-\pi/2, \pi/2]$, by inversion of $\arcsin x$; repeated "reflection across endpoints" ultimately extends $\sin t$ to a smooth, 2π-periodic function on $\mathcal{R}$.

In the complex domain, one may define a branch of $\arcsin w$ on the slit complex plane $P = \mathbb{C} \setminus \{(-\infty, -1] \cup [1, \infty)\}$ by the complex line integral: $\arcsin w = \int_0^w dr/\sqrt{1-r^2} = \int_0^1 \zeta dt/\sqrt{1-\zeta^2 t^2}$. It can be shown that $\zeta = \arcsin w$ maps P conformally onto the infinite vertical strip $V = \{w = u + iv : -\pi/2 < u < \pi/2\}$. Therefore, inversion defines $w = \sin \zeta$ as an analytic mapping of V onto P. One may then invoke the *Schwarz reflection principle*: Since $w = \sin \zeta$ approaches the real axis as ζ approaches the boundary of V, $\sin \zeta$ may be (repeatedly) extended *by reflection* to a 2π-periodic analytic function on $\mathbb{C}$.

A similar procedure yields the *lemniscatic sine function* $w = \mathrm{sl}\zeta$ (notation as in [13], §11.6), extending the function $s^{-1}(\zeta) : \mathcal{S} \to D$ introduced at the end of the last section. The important difference is that the boundary of the square $\mathcal{S}$ determines *two* "propagational directions," and the procedure leads to a *doubly periodic*, meromorphic function $\mathrm{sl} : \mathbb{C} \to \mathbb{C} \cup \{\infty\}$. Shortly, we discuss some of the most essential consequences of this construction.

But first we note that the lemniscatic integral is an *elliptic integral of the first kind* $\int \frac{dr}{\sqrt{(1-r^2)(1-mr^2)}}$, for the special parameter value $m = k^2 = -1$. Inversion of the latter integral leads to the *Jacobi elliptic sine function with modulus* k, $\mathrm{sn}(\zeta, k)$. The *elliptic cosine* $\mathrm{cn}\zeta = \sqrt{1 - \mathrm{sn}^2\zeta}$ and $\mathrm{dn}\zeta = \sqrt{1 - m\,\mathrm{sn}^2\zeta}$ are two of the other basic Jacobi elliptic functions. All such functions are doubly periodic, but the lemniscatic functions

$$\mathrm{sl}\zeta = \mathrm{sn}(\zeta, i),\ \mathrm{cl}\zeta = \sqrt{1 - \mathrm{sl}^2\zeta},\ \mathrm{dl}\zeta = \sqrt{1 + \mathrm{sl}^2\zeta} \tag{4}$$

posses additional symmetry which is essential to our story. In particular, Equations 3, 4 imply the exceptional identities:

$$\mathrm{sl}i\zeta = i\mathrm{sl}\zeta,\ \mathrm{cl}i\zeta = \mathrm{dl}\zeta,\ \mathrm{dl}i\zeta = \mathrm{cl}\zeta \tag{5}$$

It is well worth taking the time to derive further identities for $\mathrm{sl}\zeta$, "from scratch"—this we now proceed to do.

The Schwarz reflection principle allows us to extend $\mathrm{sl} : \mathcal{S} \to \mathbb{C}$ across the boundary $\partial\mathcal{S}$ according to the rule: *symmetric point-pairs map to symmetric point-pairs*. By definition, such pairs (in domain or range) are swapped by the relevant *reflection* R (antiholomorphic involution fixing boundary points). In the w-plane, we use inversion in the unit circle $R_C(w) = 1/\bar{w}$. In the $\zeta = s + it$-plane, a separate formula is required for each of the four edges making up $\partial\mathcal{S} = e_1 + e_2 + e_3 + e_4$. For e_1, we express reflection across $t = K - s$ by $R_1(\zeta) = -i\bar{\zeta} + (1 + i)K = -i\bar{\zeta} + e_+$, where we introduce the shorthand $e_\pm = (1 \pm i)K$. Then $\mathrm{sl}\zeta$ may be defined on the square $\mathcal{S}_+ = \{\zeta + e_+ : \zeta \in \mathcal{S}\}$ by the formula:

$$\mathrm{sl}\zeta = R_C \mathrm{sl} R_1 \zeta = \frac{1}{\mathrm{sl}(i\zeta + e_-)}, \quad \zeta \in \mathcal{S}_+. \tag{6}$$

$\mathcal{S}_+$ is thus mapped conformally onto the exterior of the unit circle in the Riemann sphere (extended complex plane) $\mathbb{P} = \mathbb{C} \cup \{\infty\}$, with pole $sle_+ = \infty$.

Figure 3 illustrates the extended mapping $\mathrm{sl} : \mathcal{S} \cup \mathcal{S}_+ \to \mathbb{P}$. The circular chessboard is still recognizable within the right-hand figure, though "chessboard coloring" has not been used. Instead, one of the two orthogonal families of curves has been highlighted to display the image on the right as a *topological cylinder* obtained from the Riemann sphere by removing two slits—the quarter circles in second and fourth quadrants.

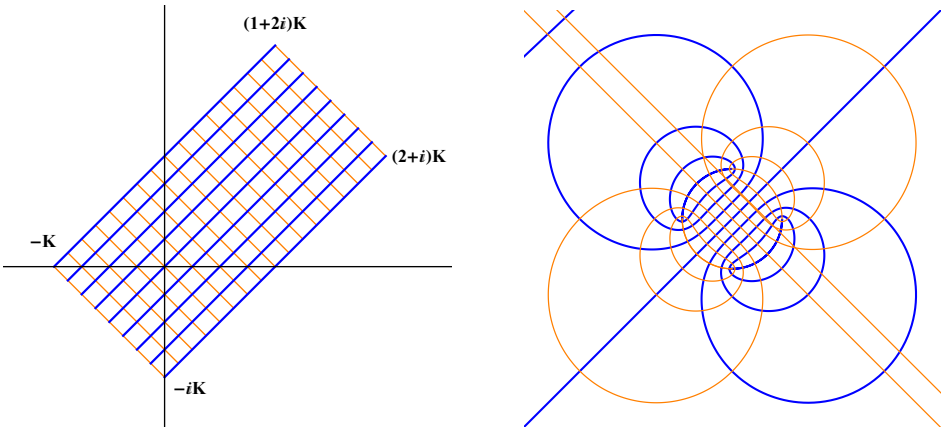

Figure 3. Mapping rectangle $\mathcal{S} \cup \mathcal{S}_+$ onto Riemann sphere by $w = \mathrm{sl}\zeta$.

We may similarly extend sl across e_2, e_3, e_4 and, by iteration, extend meromorphically to $\mathrm{sl} : \mathbb{C} \to \mathbb{P}$. The resulting extension is most conveniently described in terms of basic symmetries generated by pairs of reflections. Let $R_\pm\zeta = \pm i\bar{\zeta}$ be the reflection in the line $t = \pm s$; we use the same notation for reflections in the $w = u + iv$-plane, $R_\pm w = \pm i\bar{w}$. We may regard translations $\zeta \mapsto \zeta \pm e_+$ as composites of reflections ($R_1 R_-$ and $R_- R_1$) in parallel lines $t = K - s$ and $t = -s$,

and thus deduce the effect on $w = \mathrm{sl}\zeta$. Here we may freely apply Equation 6 as well as D_4-equivariance—which meromorphic extension of sl must respect.

Thus, $\mathrm{sl}(\zeta + e_+) = \mathrm{sl}R_1R_-\zeta = R_C\mathrm{sl}R_1R_1R_-\zeta = R_CR_-\mathrm{sl}\zeta = \frac{1}{i\mathrm{sl}\zeta}$, and identities

$$\mathrm{sl}(\zeta \pm e_+) = \frac{1}{i\mathrm{sl}\zeta}, \quad \mathrm{sl}(\zeta \pm e_-) = \frac{i}{\mathrm{sl}\zeta} \tag{7}$$

$$\mathrm{sl}(\zeta \pm 2e_\pm) = \mathrm{sl}\zeta, \tag{8}$$

$$\mathrm{sl}(\zeta \pm 2K) = \mathrm{sl}(\zeta \pm 2iK) = -\mathrm{sl}\zeta, \tag{9}$$

$$\mathrm{sl}(\zeta \pm 4K) = \mathrm{sl}(\zeta \pm 4iK) = \mathrm{sl}\zeta \tag{10}$$

follow easily in order. One should not attempt to read off corresponding identities for cl, dl using Equation 4—though we got away with this in Equation 5! (One may better appeal to angle addition formulas, to be given below.) Below, we will use the pair of equations $\mathrm{cl}(\zeta + 2K) = -\mathrm{cl}(\zeta)$ and $\mathrm{dl}(\zeta + 2K) = \mathrm{dl}(\zeta)$, which reveal the limitations of Equation 4. Actually, this points out one of the virtues of working exclusively with $\mathrm{sl}\zeta$, if possible, as it will eventually prove to be for us.

A *period* of a meromorphic function $w = f(\zeta)$ is a number $\omega \in \mathbb{C}$ such that $f(\zeta + \omega) = f(\zeta)$ for all $\zeta \in \mathbb{C}$. The *lattice of periods of* $f(\zeta)$ is the subgroup of the additive group $\mathbb{C}$ consisting of all periods of $f(\zeta)$. Let $\omega_0 = 2(1 + i)K = 2e_+ = 2ie_-$. Then the lattice of periods of $\mathrm{sl}\zeta$ is the *rescaled Gaussian integers*:

$$\Omega = \{(a + ib)\omega_0 : a, b \in \mathbb{N}\} \tag{11}$$

In fact, Equation 8 shows that any $(a + ib)\omega_0$ is a period; on the other hand, the assumption of an additional period leads quickly to a contradiction to the fact that $\mathrm{sl}\zeta$ is one-to-one on the (closed) chessboard $\mathcal{S}^c = \mathrm{closure}(\mathcal{S})$.

Using Ω, $\mathrm{sl}\zeta$ is most easily pictured by choosing a *fundamental region* for Ω and tiling the complex plane by its Ω-translates. To fit our earlier discussion, a convenient choice is the (closure of the) square consisting of four "chessboards" $\mathcal{R} = \mathcal{S} \cup \mathcal{S}_+ \cup \mathcal{S}_- \cup \mathcal{S}_\pm$, where $\mathcal{S}_- = \{\zeta + e_- : \zeta \in \mathcal{S}\}$, $\mathcal{S}_\pm = \{\zeta + 2K : \zeta \in \mathcal{S}\}$. To say that $\mathcal{R}^c$ is a fundamental region means:

(1) Any $\zeta \in \mathbb{C}$ is equivalent to some $\zeta_0 \in \mathcal{R}^c$ in the sense that $\zeta - \zeta_0 \in \Omega$.
(2) No two elements in $\mathcal{R} = \mathrm{interior}(\mathcal{R}^c)$ are equivalent.

The double periodicity of $\mathrm{sl}\zeta$ is realized concretely in terms of the square tiling; $\mathrm{sl}\zeta$ maps $\mathcal{R}$ two-to-one onto $\mathbb{P}$, and repeats itself identically on every other tile.

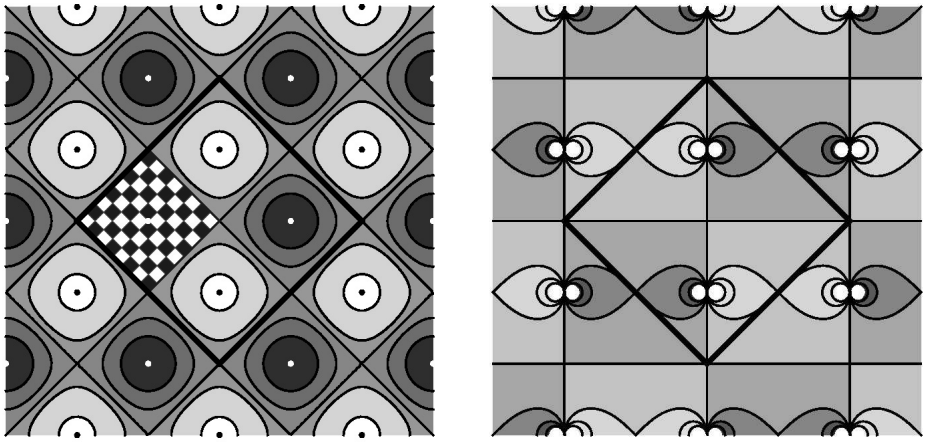

Figure 4. Contour plots of $|\mathrm{sl}\zeta|$ (left) and $\mathrm{Im}[\mathrm{sl}\zeta]$ (right).

The left side of Figure 4 illustrates the behavior just described using a contour plot of $|\mathrm{sl}z|$ (with tile $\mathcal{R}$ and chessboard subtile $\mathcal{S}$ superimposed). The critical level set $|\mathrm{sl}\zeta| = 1$ is recognizable as a square grid; half of the squares contain zeros (white dots), the other half contain poles (black dots). The right side of Figure 4 is a contour plot of $\mathrm{Im}[\mathrm{sl}\zeta]$. The level set $\mathrm{Im}[\mathrm{sl}\zeta] = 0$ is a larger square grid, this time formed by vertical and horizontal lines. We note that such a plot by itself (without superimposed tile $\mathcal{R}$) is visually misleading as to the underlying lattice.

A closely related idea is to regard $\mathrm{sl}\zeta$ as a function on the quotient $T^2 = \mathbb{C}/\Omega$—topologically, the torus obtained from the square $\mathcal{R}^c$ by identifying points on opposite edges (using $\zeta + i^k\omega_0 \equiv \zeta$). Then $\mathrm{sl} : T^2 \to \mathbb{P}$ is a *double branched cover* of the Riemann sphere by the torus. This point of view meshes perfectly with our earlier description of $\mathrm{sl} : \mathcal{S} \cup \mathcal{S}_+ \to \mathbb{P}$ as defining a cylinder. For the same description applies to the other *sheet* $\mathrm{sl} : \mathcal{S}_- \cup \mathcal{S}_\pm \to \mathbb{P}$, and the two identical sheets "glue" together along the *branch cuts* (quarter-circle slits) to form a torus T^2.

Yet another point of view uses the basic differential equation satisfied by $r = \mathrm{sl}s$. Applying the inverse function theorem to $\frac{ds}{dr} = 1/\sqrt{1-r^4}$ gives

$$(\frac{dr}{ds})^2 = 1 - r^4 \tag{12}$$

Here we have temporarily reverted to our original real notation, but it should be understood that Equation 12 is valid in the complex domain; r may be replaced by w and s by ζ. Also, we note that the equation implies the following derivative formulas for the lemniscatic functions:

$$\frac{d}{d\zeta}\mathrm{sl}\zeta = \mathrm{cl}\zeta\mathrm{dl}\zeta, \quad \frac{d}{d\zeta}\mathrm{cl}\zeta = -\mathrm{sl}\zeta\mathrm{dl}\zeta, \quad \frac{d}{d\zeta}\mathrm{dl}\zeta = \mathrm{sl}\zeta\mathrm{cl}\zeta \tag{13}$$

In particular, $\frac{d}{d\zeta}\mathrm{sl}\zeta$ vanishes at the chessboard corners $\pm K, \pm iK$, where the mapping of Figure 3 folds the long edges of the rectangle $\mathcal{S} \cup \mathcal{S}_+$ onto *doubled* quarter circles; these four critical points account for the branching behavior of $\mathrm{sl} : T^2 \to \mathbb{P}$.

In effect, $\mathrm{sl}\zeta$ defines a local coordinate on T^2, but is singular at the four points just mentioned. Actually, $\mathrm{sl}\zeta$ may be regarded as the first of two coordinates in a nonsingular parameterization of the torus. Here it is helpful to draw again on the analogy with $x = \sin t$ as a coordinate on the unit circle and the differential equation $(\frac{dx}{dt})^2 = 1 - x^2$. Just as the circle $x^2 + y^2 = 1$ is parameterized by $x = \sin t$, $y = \cos t$ ($t = \pi/2 - \theta$), the above formulas lead us to parameterize a quartic algebraic curve:

$$y^2 = 1 - x^4; \quad x = \mathrm{sl}\zeta,\ y = \mathrm{cl}\zeta\ \mathrm{dl}\zeta \tag{14}$$

This curve is in fact an *elliptic curve*—it is modeled on T^2—and we have effectively described its underlying analytic structure as a *Riemann surface of genus one*.

4. Parameterization of the lemniscate

In the previous two sections we developed the lemniscatic functions by way of two important applications; one a conformal mapping problem, the other a parameterization of an elliptic curve. The lemniscatic functions may also be used, fittingly enough, to neatly express arclength parameterization of the lemniscate $\mathcal{B}$ itself:

$$x(s) = \frac{1}{\sqrt{2}}\mathrm{dl}s\ \mathrm{sl}s,\ y(s) = \frac{1}{\sqrt{2}}\mathrm{cl}s\ \mathrm{sl}s,\ 0 \le s \le 4K \tag{15}$$

Equations 4 imply that $x = x(s), y = y(s)$ satisfy $(x^2 + y^2)^2 = x^2 - y^2$; further, Equations 13 lead to $x'(s)^2 + y'(s)^2 = 1$, as required. We note that s may be replaced by complex parameter ζ, as in Equation 14, for global parameterization of $\mathcal{B}$ as complex curve.

But first we focus on real points of $\mathcal{B}$ and subdivision of the plane curve into equal arcs. As a warmup, observe that Gauss's theorem on regular n-gons may be viewed as a result about constructible values of the sine function. For if n is an integer such that $y = \sin\frac{\pi}{2n}$ is a constructible number, so is $x = \cos\frac{\pi}{2n} = \sqrt{1 - y^2}$ constructible; then all points $(\sin\frac{\pi j}{2n}, \cos\frac{\pi j}{2n}),\ j = 1 \ldots 4n$ are constructible by virtue of the angle addition formulas for sine and cosine.

Likewise, Abel's result on uniform subdivision of the lemniscate is about constructible values $\mathrm{sl}(\frac{K}{n})$. For if it is known that a *radius* $r(K/n) = \mathrm{sl}(K/n)$ is a constructible number, it follows from Equation 15 that the corresponding point $(x(K/n),\ y(K/n))$ on $\mathcal{B}$ is constructible. Further, in terms of $r(K/n)$, $x(K/n)$, $y(K/n)$, only rational operations are required to divide the lemniscate into $4n$ arcs of length K/n (or n arcs of length $4K/n$). Specifically, one can compute the values $r(jK/n), x(jK/n), y(jK/n)$, $j = 1, \ldots, n$, using the *angle addition formulas for lemniscatic functions*:

$$\mathrm{sl}(\mu+\nu) = \frac{\mathrm{sl}\mu\,\mathrm{cl}\nu\,\mathrm{dl}\nu + \mathrm{sl}\nu\,\mathrm{cl}\mu\,\mathrm{dl}\mu}{1+\mathrm{sl}^2\mu\,\mathrm{sl}^2\nu} \tag{16}$$

$$\mathrm{cl}(\mu+\nu) = \frac{\mathrm{cl}\mu\,\mathrm{cl}\nu - \mathrm{sl}\mu\,\mathrm{sl}\nu\,\mathrm{dl}\mu\,\mathrm{dl}\nu}{1+\mathrm{sl}^2\mu\,\mathrm{sl}^2\nu} \tag{17}$$

$$\mathrm{dl}(\mu+\nu) = \frac{\mathrm{dl}\mu\,\mathrm{dl}\nu + \mathrm{sl}\mu\,\mathrm{sl}\nu\,\mathrm{cl}\mu\,\mathrm{cl}\nu}{1+\mathrm{sl}^2\mu\,\mathrm{sl}^2\nu} \tag{18}$$

(We note that the general angle addition formulas for the elliptic functions $\mathrm{sn}\zeta = \mathrm{sn}(\zeta,k), \mathrm{cn}\zeta = \mathrm{cn}(\zeta,k), \mathrm{dn}\zeta = \mathrm{dn}(\zeta,k)$ are very similar; the denominators are $1-k^2\mathrm{sn}^2\mu\,\mathrm{sn}^2\nu$ and the third numerator is $\mathrm{dn}\mu\,\mathrm{dn}\nu - k^2\mathrm{sn}\mu\,\mathrm{sn}\nu\,\mathrm{cn}\mu\,\mathrm{cn}\nu$.)

Everything so far seems to build on the analogy: *The lemniscatic sine function is to the lemniscate as the circular sine function is to the circle.*

But the moment we turn to constructibility of *complex points* on $\mathcal{B}$, an interesting difference arises: The integer j in the above argument can be replaced by a Gaussian integer $j+ik$. That is, one may use $\mu = jK/n, \nu = ikK/n$ in Equations 16-18, then apply Equations 5, then reduce integer multiple angles as before. Thus, a single constructible value $r(K/n) = \mathrm{sl}(K/n)$ ultimately yields n^2 constructible values $r((j+ik)K/n),\ 0 < j,k \le n$—hence n^2 points $(x((j+ik)K/n), y((j+ik)K/n)$ on $\mathcal{B}$ (actually four times as many points, but the remaining points are easily obtained by symmetry anyway).

Two remarks are in order here:

(1) No such phenomenon holds for the circle. Note that $(\sin\pi, \cos\pi) = (0,-1)$ is a constructible point on the real circle, while $(\sin i\pi, \cos i\pi)$ is a *non-constructible* point on the complex circle—otherwise, the transcendental number $e^\pi = \cos i\pi - i\sin i\pi$ would also be constructible!

(2) The constructibility of $r(K/n)$, $n = 2^j p_1 p_2 \ldots p_k$, may be viewed as an *algebraic consequence* of its congruence class of n^2 values!

Though both remarks are interesting from the standpoint of algebra or number theory—in fact they belong to the deeper aspects of our subject—statements about complex points on a curve may be harder to appreciate geometrically. However, beautiful visualizations of such points may be obtained by *isotropic projection* onto the real plane $\mathbb{R}^2 \simeq \mathbb{C}$: $(x_0, y_0) \mapsto z_0 = x_0 + iy_0$. (The geometric meaning of this projection is not so different from stereographic projection: Point $(x_0, y_0) \in \mathbb{C}^2$ lies on a complex line $x+iy = z_0$ through the *circular point* c_+ with homogeneous coordinates $[1, i, 0]$, and the projection of (x_0, y_0) from c_+ is the point of intersection $(\mathrm{Re}[z_0], \mathrm{Im}[z_0])$ of line $x+iy = z_0$ and real plane $\mathrm{Im}[x] = \mathrm{Im}[y] = 0$.)

In particular, the (complexified) arclength parameterization $\Gamma(\zeta) = (x(\zeta), y(\zeta))$ of the lemniscate thus results in a meromorphic function on $\mathbb{C}$,

$$\gamma(\zeta) = x(\zeta) + iy(\zeta) = \frac{1}{\sqrt{2}}\mathrm{sl}\zeta\ (\mathrm{dl}\zeta\ + i\mathrm{cl}\zeta),\ \zeta \in \mathbb{C}, \tag{19}$$

by which we will plot, finally, the *lemniscate parallels* alluded to in the introduction: $\gamma(s+it_0),\ -2K \le s \le 2K,\ t_0 \in \mathbb{R}$. For instance, Figure 5 shows lemniscate parallels for the uniformly spaced "time"-values $t_0 = jK/4,\ -4 \le j < 4$.

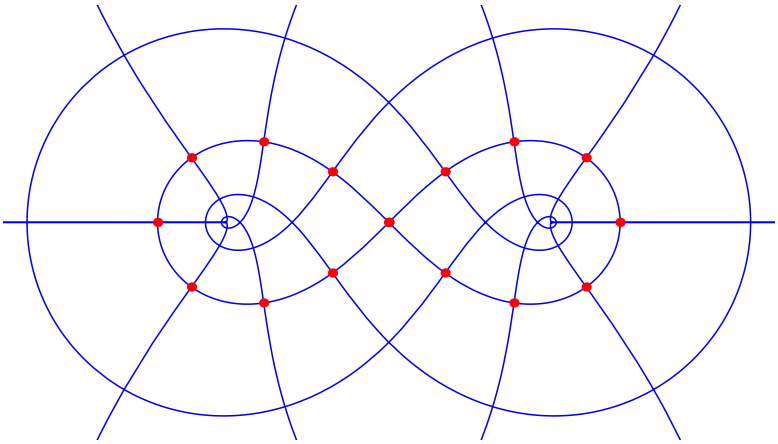

Figure 5. Lemniscate parallels for times $t_0 = \frac{jK}{4},\ -4 \le j < 4$.

Figure 5 is but a more complete version of Figure 1, but this time we are in a position to explain some of the previously mysterious features of the figure. The following statements apply not only to Figure 5 but also to similar plots obtained using Equation 19:

- The family of lemniscate parallels is *self-orthogonal*.
- The time increment Δt induces an equal curve increment Δs.
- For $\Delta t = K/n$, $n = 2^j p_1 p_2 \dots p_k$, all intersections are constructible.

To explain the first two statements we combine Equations 5, 9 and above mentioned identities $\mathrm{cl}(\zeta + 2K) = -\mathrm{cl}(\zeta), \mathrm{dl}(\zeta + 2K) = \mathrm{dl}(\zeta)$ to obtain $\gamma(i\zeta) = \frac{1}{\sqrt{2}}\mathrm{sl}(i\zeta)(\mathrm{dl}(i\zeta) + i\mathrm{cl}(i\zeta)) = \frac{1}{\sqrt{2}}\mathrm{sl}(\zeta)(-\mathrm{dl}(\zeta) + i\mathrm{cl}(\zeta)) = \gamma(\zeta + 2K)$, hence:

$$\gamma(s + it) = \gamma(i(t - is)) = \gamma(t + 2K - is) \tag{20}$$

Thus, the γ-images of vertical lines $s = s_0$ and horizontal lines $t = t_0$ are one and the same family of curves! Since γ preserves orthogonality, the first claim is now clear. By the same token, since members of the family are separated by uniform time increment Δt, they are likewise separated by uniform s-increment. In particular, curves in the family divide the lemniscate into 16 arcs of equal length. (The last bulleted statement is a part of a longer story for another day!).

5. Squaring the sphere

The meromorphic lemniscate parameterization $\gamma(\zeta)$ arose, over the course of several sections, in a rather *ad hoc* manner. Here we describe a more methodical derivation which leads to a somewhat surprising, alternative expression for γ as a composite of familiar geometric mappings. Ignoring linear changes of variable,

the three required mappings are: The lemniscatic sine $\mathrm{sl}\, z$, the *Joukowski map* $j(z)$, and the complex reciprocal $\iota(z) = 1/z$. The idea is to use j to parameterize the hyperbola $\mathcal{H}$, apply ι to turn $\mathcal{H}$ into $\mathcal{B}$, then compute the reparametrizing function required to achieve unit speed.

First recall the Joukowski map

$$j(z) = \frac{1}{2}(z + \frac{1}{z}), \tag{21}$$

a degree two map of the Riemann sphere with ramification points $\pm 1 = j(\pm 1)$; the unit circle is mapped two-to-one to the interval $[-1, 1]$, and the interior/exterior of the unit disk is mapped conformally onto the slit plane $\mathbb{C} \setminus [-1, 1]$. (Joukowski introduced j to study fluid motion around airfoils, building on the simpler flow around obstacles with circular cross sections.)

We note also that j maps circles $|z| = r$ to confocal ellipses (degenerating at $r = 1$) and rays $\mathrm{Arg}\, z = const$ to (branches of) the orthogonal family of confocal hyperbolas. In particular, $\mathrm{Arg}\, z = \pi/4$ is mapped by j to the rectangular hyperbola with foci ± 1: $x^2 - y^2 = 1/2$. We rescale to get $\mathcal{H}$, then take reciprocal: $\mathcal{B}$ is the image of the line $\mathrm{Re}[z] = \mathrm{Im}[z]$ under the map

$$\beta(z) = \iota(\sqrt{2} j(z)) = \frac{\sqrt{2} z}{1 + z^2} \tag{22}$$

(Inversion in the unit circle, discussed earlier, is given by conjugate reciprocal $z \mapsto 1/\bar{z}$; but by symmetry of $\mathcal{H}$, ι yields the same image.)

Let $\sigma = \sigma_8 = e^{\pi k i/4}$. Taking real and imaginary parts of $\beta(\sigma t) = \beta(\frac{1+i}{\sqrt{2}} t)$ results in the following parameterization of the real lemniscate:

$$x(t) = \frac{t + t^3}{1 + t^4}, \quad y(t) = \frac{t - t^3}{1 + t^4} \tag{23}$$

This rational parameterization possess beautiful properties of its own, but our current agenda requires only to relate its arclength integral to the lemniscatic integral by simple (complex!) substitution $t = \sigma\tau$:

$$s(t) = \int \sqrt{x'(t)^2 + y'(t)^2}\, dt = \int \frac{\sqrt{2}}{\sqrt{1 + t^4}}\, dt = \int \frac{\sqrt{2}\sigma}{\sqrt{1 - \tau^4}}\, d\tau \tag{24}$$

Thus we are able to invert $s(t)$ via the lemniscatic sine function, put $t = t(s)$ in $\beta(\sigma t)$, and simplify with the help of Equation 5: $\gamma(s) = \beta(\sigma t(s)) = \beta(i\mathrm{sl}\, \frac{s}{\sqrt{2}\sigma}) = \beta(\mathrm{sl}\, \frac{\sigma}{\sqrt{2}} s)$.

We are justified in using the same letter γ, as in Equation 19, to denote the resulting meromorphic arclength parameterization:

$$\gamma(\zeta) = \beta(\mathrm{sl}(\frac{\sigma}{\sqrt{2}}\zeta)) = \frac{\sqrt{2}\, \mathrm{sl}(\frac{1+i}{2}\zeta)}{1 + \mathrm{sl}^2(\frac{1+i}{2}\zeta)} \tag{25}$$

Comparing this expression with Equation 19, one could not be expected to recognize that these meromorphic functions are one and the same; but both satisfy $\gamma(0) = 0, \gamma'(0) = \sigma$—so it must be the case! (It requires a bit of work to verify this directly with the help of elliptic function identities.)

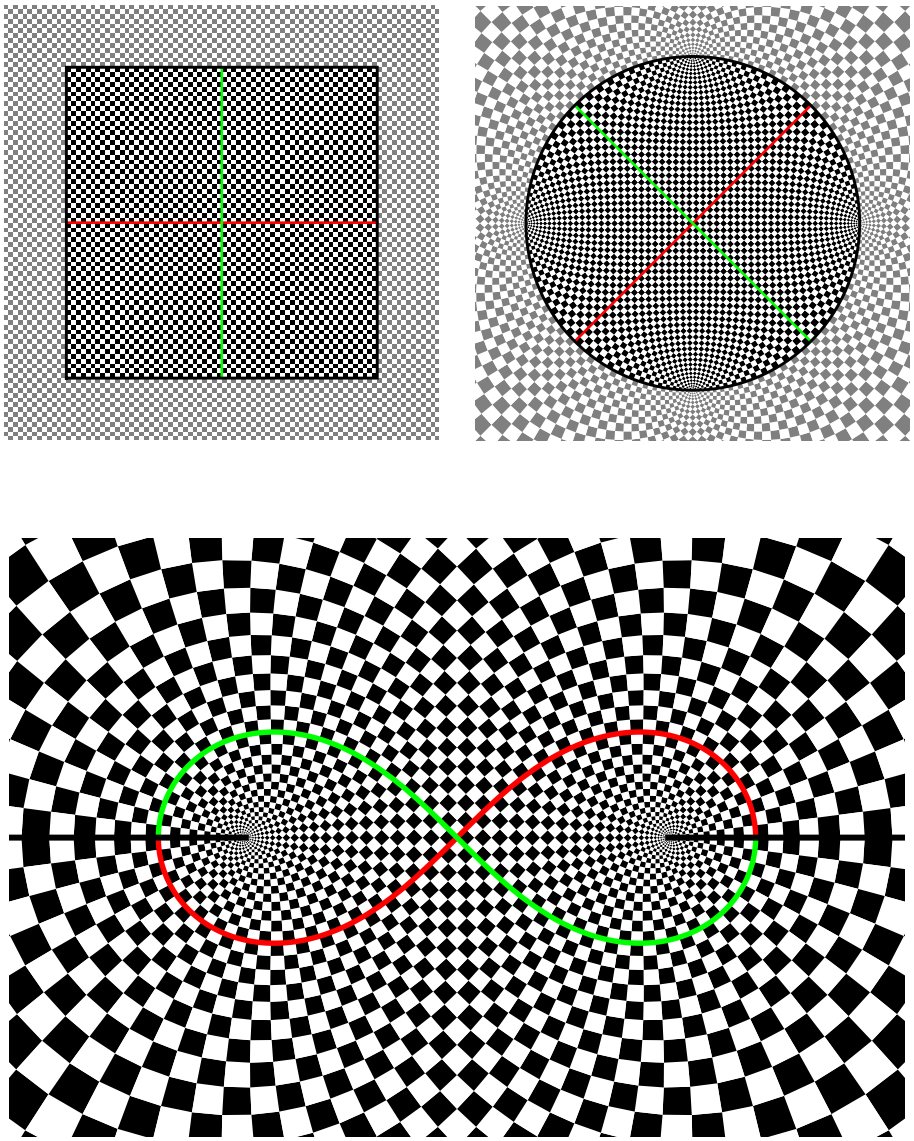

Figure 6. The factorization $\gamma(\zeta) = \beta(\mathrm{sl}(\frac{\sigma}{\sqrt{2}}\zeta))$: From square to round to lemniscatic chessboards.

Figure 6 illustrates the factorization $\gamma(\zeta) = \beta(\mathrm{sl}(\frac{\sigma}{\sqrt{2}}\zeta))$ with the aid of black and white $n \times n$ "chessboards" in domain, intermediate, and target spaces. (Though it may be more meaningful to speak of $n \times n$ "checkers" or "draughts," we have reason shortly to prefer the chess metaphor.) The present choice $n = 64$ is visually representative of integers $n >> 8$, but belongs again to the algebraically simplest class $n = 2^k$. The square board (SB) in the domain has corners $(\pm 1 \pm i)K$ (upper left). Rotation by $\pi/4$ and dilation by $\sqrt{2}$ takes SB to the square $\mathcal{S}$, which was

earlier seen to be mapped conformally onto the unit disc by $\mathrm{sl}\, z$. The result is the round board (RB) in the intermediate space (upper right).

The *lemniscatic chess board* (bottom) is the conformal image $LB = \gamma(SB) = \beta(RB)$. As a domain, LB occupies the slit plane $\mathbb{C} \setminus \mathcal{I}$, $\mathcal{I} = (-\infty, -1/\sqrt{2}] \cup [1/\sqrt{2}, \infty)$. Note that the closure of LB is the sphere $LB^c = \gamma(SB^c) = \mathbb{P}$—so γ^{-1} *squares the sphere!* In the process, the horizontal (red) and vertical (green) centerlines on SB are carried by γ to the two halves of the real lemniscate in LB. (For n even, the lemniscate is already a "gridline" of LB.)

In addition to providing a more geometric interpretation for $\gamma(\zeta)$, Equation 25 represents an improvement over Equation 19 with respect to "number theory and numerics of LB." Here it's nice to consider discrete versions of RB and LB: Let each of the n^2 curvilinear squares be replaced by the quadrilateral with the same vertices. (This is in fact how the curvilinear squares in Figure 6 are rendered! Such a method reduces computation considerably and provides much sharper graphical results.) With this interpretation, we note that only rational operations are required to construct LB from RB.

6. Lemniscatic chess

In Figure 6 one detects yet unfinished business. What became of the gray and white checkered regions exterior to SB and RB? What to make of checks of the same color meeting along $\mathcal{I}$ in LB? For any n, symmetry forces this coloring *faux pas.* Something appears to be missing!

For amusement, let's return to case $n = 8$ and the spherical chessboard LB. Observe that in the game of lemniscatic chess, a bishop automatically changes from white to black or black to white each time he crosses $\mathcal{I}$. From the bishop's point of view, the board seems twice as big, since a neighborhood on LB feels different, depending on whether he's white or black.

In effect, the bishop's wanderings define a Riemann surface Σ, consisting of two oppositely colored, but otherwise identical, copies of LB, joined together along $\mathcal{I}$ to form a chessboard of $2n^2 = 128$ squares. In fact, it will be seen that Σ—itself a copy of the Riemann sphere $\Sigma \simeq \mathbb{P}$—may be regarded as the underlying Riemann surface, the intrinsic analytical model, of the algebraic curve $\mathcal{B}$.

To approach this from a slightly different angle, we note that $\mathcal{B}$ is a rational curve; its parameterization $b(t) = (x(t), y(t))$ given by Equation 23 shows that the totality of its (real, complex, and infinite) points may be identified with the space of parameter values $t \in \mathbb{P}$. In other words, $\mathcal{B}$ has *genus zero*. In declaring $\mathcal{B} \simeq \mathbb{P} = \Sigma$, the double point at the origin is treated as two separate points, $b(0), b(\infty)$, one for each *branch* of $\mathcal{B}$. Likewise, the lemniscate's four ideal points are double circular points $c_\pm$: $b(\sigma^3), b(\sigma^7)$, and $b(\sigma), b(\sigma^5)$. ($\mathcal{B}$ is said to be a *bicircular curve*.)

To understand the relationship between the two descriptions of Σ is to glimpse the beauty of isotropic coordinates, $z_1 = x + iy, z_2 = x - iy$. In these coordinates, $x = \frac{z_1+z_2}{2}, y = \frac{z_1-z_2}{2i}$ and the equation for $\mathcal{B}$ may be re-expressed $0 = f(x, y) = g(z_1, z_2) = z_1^2 z_2^2 - \frac{1}{2}(z_1^2 + z_2^2)$. A similar computation (which

proves to be unnecessary) turns Equation 23 into a rational parameterization of $\mathcal{B}$ in isotropic coordinates, $(z_1(t), z_2(t))$.

To illustrate a general fact, we wish to express $(z_1(t), z_2(t))$ in terms of our original complex parameterization $z_1(t) = \beta(\sigma t)$. Let the *conjugate* of an analytic function $h(z)$ defined on U be the analytic function on $\bar{U}$ obtained by "complex conjugation of coefficients," $\bar{h}(z) = \overline{h(\bar{z})}$. For example, $\bar{\beta} = \beta$, consequently $h(z) = \beta(\sigma z)$ has conjugate $\bar{h}(z) = \beta(\zeta/\sigma)$. Now it is a fact that the corresponding parameterization of the complex curve $\mathcal{B}$ may be expressed simply:

$$z \mapsto (z_1(z), z_2(z)) = (h(z), \bar{h}(z)) = (\beta(\sigma z), \beta(z/\sigma)) \tag{26}$$

Given this parameterization, on the other hand, isotropic projection $(z_1, z_2) \mapsto z_1$ returns the original complex function $h(z) = \beta(\sigma z)$.

Now we've come to the source of the doubling: Isotropic projection determines a $2-1$ meromorphic function $\rho : \mathcal{B} \to \mathbb{P}$. Recall each isotropic line $z_1 = x_0 + iy_0$ meets the fourth degree curve $\mathcal{B}$ four times, counting multiplicity. Each such line passes through the double circular point $c_+ \in \mathcal{B}$, and the two finite intersections with $\mathcal{B}$ give rise to the two sheets of the isotropic image. Two exceptional isotropic lines are tangent to $\mathcal{B}$ at c_+, leaving only one finite intersection apiece; the resulting pair of projected points are none other than the foci of the lemniscate.

The same principles apply to the arclength parameterization. To cover $\mathcal{B}$ once, the parameter ζ may be allowed to vary over the *double chessboard* $2SR$ occupying the rectangle $-K \le \mathrm{Re}[\zeta] < 3K$, $-K \le \mathrm{Im}[\zeta] < K$. While $\gamma(\zeta)$ maps $2SR$ *twice* onto LB (according to the symmetry $\gamma(\zeta + 2K) = \gamma(i\zeta)$), the corresponding parameterization $(\gamma(\zeta), \bar{\gamma}(\zeta)) = (\beta(\mathrm{sl}(\frac{\sigma}{\sqrt{2}}\zeta)), \beta(\mathrm{sl}(\frac{1}{\sqrt{2}\sigma}\zeta))$ maps $2SR$ once onto the bishop's world—$\mathcal{B}$ divided into 128 squares. Note that this world is modeled by the full intermediate space (Figure 6, upper right), in which there are four "3-sided squares," but no longer any adjacent pairs of squares of the same color.

7. A tale of two tilings

By now it will surely have occurred to the *non-standard chess* enthusiast that the board may be doubled once again to the torus T^2 modeled by the fundamental square $4SR$: $-K \le \mathrm{Re}[\zeta],\ \mathrm{Im}[\zeta] < 3K$. That is to say that LS (Figure 6, bottom) is *quadruply* covered by the elliptic curve Equation 14, which is itself infinitely covered by $\mathbb{C}$.

Thus, we have worked our way back to $\mathbb{C}$—the true *starting point*. Be it double, quadruple or infinite coverings, our images have displayed transference of structure *forwards*. A common thread and graphical theme, in any event, has been the hint or presence of square tiling of the plane and $*442$ *wallpaper symmetry* (see [2] to learn all about symmetry, tiling, and its notation). Likewise for subdivision of the lemniscate, the underlying symmetry and algebraic structure derive from $\mathbb{C}$ and the Gaussian integers; the intricate consequences are the business of Galois theory, number theory, elliptic functions—stories for another time ([11], [3], [9]).

It may sound strange, then: The symmetry group of the lemniscate itself, as a projective algebraic curve, is the octahedral group $O \simeq S_4$, the $*432$ tiling of the

sphere (see Figure 7) is the skeleton of the lemniscate's intrinsic geometry. Projective O-symmetry characterizes $\mathcal{B}$ among genus zero curves of degree at most four ([7]). The natural Riemannian metric on $\mathcal{B} \subset \mathbb{C}P^2$ has precisely nine geodesics of reflection symmetry, which triangulate $\mathcal{B}$ as a disdyakis dodecahedron (which has 26 vertices, 72 edges and 48 faces); the 26 polyhedral vertices are the critical points of Gaussian curvature K ([8]). These are: 6 maxima $K = 2$, 8 minima $K = -7$ and 12 saddles $K = -1/4$, which are, respectively, the centers of 4-fold, 3-fold, and 2-fold rotational symmetry. It is also the case that our rational parameterization of $\mathcal{B}$ (given by Equation 23 or 26) realizes the full octahedral ($*432$) symmetry. (The 48-element *full octahedral group* O_h is distinct from the 48-element *binary octahedral group* $2O$, which is related to O like the bishop's world to LB—again another story.)

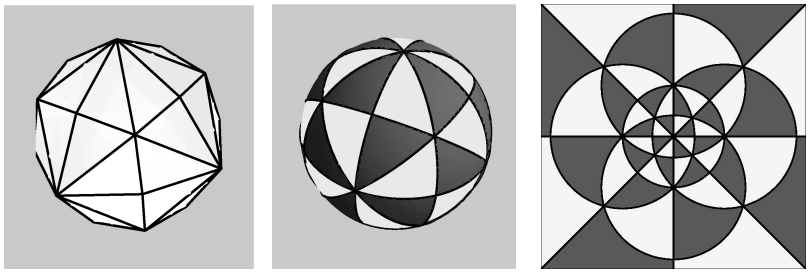

Figure 7. The disdyakis dodecahedron, $*432$ spherical tiling, and its stereographic planar image.

It is indeed a curious thing that these planar and spherical tilings and their symmetries somehow coexist in the world of the lemniscate. In an effort to catch both in the same place at the same time, we offer two final images, Figure 8. The idea here is to reverse course, transferring structure *backwards*—from lemniscate $\mathcal{B}$ to torus T^2—via the $2-1$ map $\gamma : T^2 \to \mathbb{P}$. On the left, the $*432$ spherical tiling is pulled back; on the right, a contour plot of K is pulled back. In both cases, we have chosen (for aesthetic reasons) to indicate a *wallpaper pattern* meant to fill the whole plane; however, for the discussion to follow, it should be kept in mind that T^2 is represented by the *central* 2×2 *square* in each (4×4) figure.

From a purely topological point of view, Figures 7 (middle) and 8 (left) together provide a perfect illustration of the proof of the *Riemann-Hurwitz Formula*: If $f : M \to N$ is a branched covering of Riemann surfaces, f has degree n and b branch points (counting multiplicities), and χ denotes Euler characteristic of a surface, then $\chi(M) = n\chi(N) - r$. Here we take $N = \mathbb{P}$, triangulated as in the former figure ($\chi(N) = V - E + F = 26 - 72 + 48 = 2$), and $M = T^2$ with triangulation pulled back from N by $f(\zeta) = \mathrm{sl}(\frac{1+i}{2}\zeta)$. Within T^2, f has four first order *ramification points*, where f fails to be locally $1-1$; these are the points where 16 curvilinear triangles meet. The mapping f doubles the angles $\pi/8$ of these triangles and wraps neighborhoods of such points twice around respective image points $\pm 1, \pm i \in \mathbb{P}$ (together with $0, \infty \in \mathbb{P}$, these may be identified as the "octahedral vertices" in

Figure 7, right). Since $f : T^2 \to \mathbb{P}$ has degree two, the resulting triangulation of T^2 has double the vertices, edges, and faces of PL, except for the vertices at ramification points which correspond one-to-one. Therefore, $\chi(T^2) = 2\chi(PL) - 4 = 0$, just as it should.

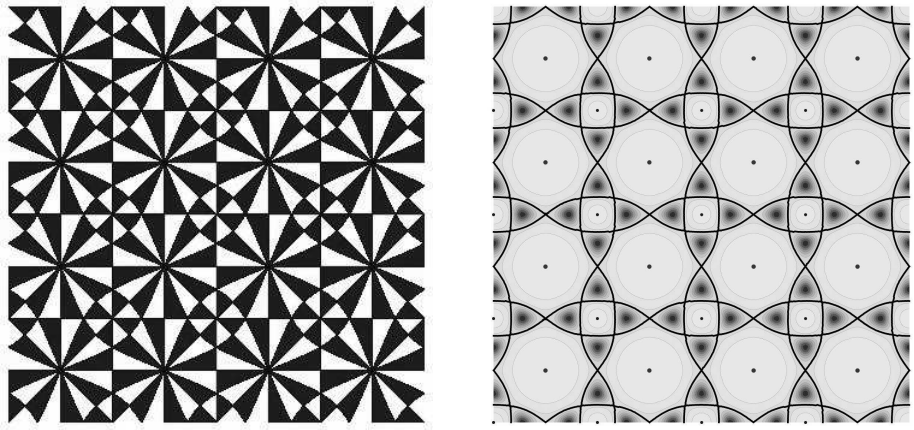

Figure 8. Wallpaper preimages of triangulated lemniscate (left) and lemniscate's curvature (right).

One may wish to contemplate the more subtle relationship between symmetries of the triangulated torus and those of the sphere. The group G of orientation-preserving (*translational* and *rotational*) symmetries of the former has order $|G| = 16$. To account for the smaller number $|G| < |O| = 24$, note that f breaks octahedral symmetry by treating the (unramified) points $0, \infty \in \mathbb{P}$ unlike $\pm 1, \pm i \in \mathbb{P}$. The former correspond to the four points in T^2 (count them!) where 8 triangles meet. But neither can all elements of G be "found" in O. Imagine a chain of "stones" $s_0, s_1, s_2, \ldots$ (vertices $s_j \in \mathbb{P}$), with $s_{j+1} = r_j s_j$ obtained by applying $r_j \in O$, and the corresponding chain of stones in $T^2 \ldots$ Anyone for a game of *disdyakis dodecahedral Go?*

References

[1] A.B. Basset, *An Elementary Treatise on Cubic and Quartic Curves*, Merchant Books, 2007.

[2] J. H. Conway, H. Burgiel and C. Goodman-Strauss, *The symmetries of things*, A. K. Peters, LTD, 2008.

[3] D. Cox and J. Shurman, Geometry and number theory on clovers, *Amer. Math. Monthly*, 112 (2005) 682–704.

[4] H. Hilton, *Plane Algebraic Curves, second edition*, London, Oxford University Press, 1932.

[5] F. Klein, *The icosahdron and the solution of equations of the fifth degree*, Dover Publications, 1956.

[6] J. Langer and D. Singer, Foci and foliations of real algebraic curves, *Milan J. Math.*, 75 (2007) 225–271.

[7] J. Langer and D. Singer, When is a curve an octahedron?, *Amer. Math. Monthly*, 117 (2010) 889–902.

[8] J. Langer and D. Singer, Reflections on the lemniscate of Bernoulli: The forty eight faces of a mathematical gem, *Milan J. Math.*, 78 (2010) 643–682.
[9] J. Langer and D. Singer, From square to round by geometric means, preprint, 2011.
[10] V. Prasolov and Y. Solovyev, *Elliptic Functions and Elliptic Integrals*, Translations of Mathematical Monographs, Vol. 170, 1997. American Mathematical Society.
[11] M. Rosen, Abel's theorem on the lemniscate, *Amer. Math. Monthly*, 88 (1981) 387–395.
[12] G. Salmon, *A Treatise on the Higher Plane Curves, Third Edition*, G. E. Stechert & Co., New York, 1934.
[13] J. Stillwell, *Mathematics and Its History*, 2nd ed., Springer, 2002.
[14] Zwikker C. Zwikker, *The Advanced Geometry of Plane Curves and their Applications*, Dover Publications, 1963.

Joel C. Langer: Department of Mathematics, Case Western Reserve University, Cleveland, Ohio 44106-7058, USA
E-mail address: joel.langer@case.edu

David A. Singer: Department of Mathematics, Case Western Reserve University, Cleveland, Ohio 44106-7058, USA
E-mail address: david.singer@case.edu